



## OPEN ACCESS

## EDITED BY

Govind Nair,  
National Institutes of Health (NIH),  
United States

## REVIEWED BY

Dingding Shen,  
Shanghai Jiao Tong University, China  
Yufen Jennie Chen,  
Northwestern University, United States

## \*CORRESPONDENCE

Giovanni Schifitto  
✉ giovanni\_schifitto@urmc.rochester.edu

<sup>†</sup>These authors have contributed equally to this work and share first authorship

RECEIVED 14 June 2023

ACCEPTED 14 August 2023

PUBLISHED 31 August 2023

## CITATION

Singh MV, Uddin MN, Singh VB, Peterson AN, Murray KD, Zhuang Y, Tyrell A, Wang L, Tivarus ME, Zhong J, Qiu X and Schifitto G (2023) Initiation of combined antiretroviral therapy confers suboptimal beneficial effects on neurovascular function in people with HIV.  
*Front. Neurol.* 14:1240300.  
doi: 10.3389/fneur.2023.1240300

## COPYRIGHT

© 2023 Singh, Uddin, Singh, Peterson, Murray, Zhuang, Tyrell, Wang, Tivarus, Zhong, Qiu and Schifitto. This is an open-access article distributed under the terms of the [Creative Commons Attribution License \(CC BY\)](https://creativecommons.org/licenses/by/4.0/). The use, distribution or reproduction in other forums is permitted, provided the original author(s) and the copyright owner(s) are credited and that the original publication in this journal is cited, in accordance with accepted academic practice. No use, distribution or reproduction is permitted which does not comply with these terms.

# Initiation of combined antiretroviral therapy confers suboptimal beneficial effects on neurovascular function in people with HIV

Meera V. Singh<sup>1,2†</sup>, Md Nasir Uddin<sup>1,3†</sup>, Vir B. Singh<sup>4</sup>, Angelique N. Peterson<sup>1</sup>, Kyle D. Murray<sup>5</sup>, Yuchuan Zhuang<sup>6</sup>, Alicia Tyrell<sup>7</sup>, Lu Wang<sup>8</sup>, Madalina E. Tivarus<sup>9,10</sup>, Jianhui Zhong<sup>3,9,10</sup>, Xing Qiu<sup>8</sup> and Giovanni Schifitto<sup>1,6,9\*</sup>

<sup>1</sup>Department of Neurology, University of Rochester, Rochester, NY, United States, <sup>2</sup>Department of Microbiology and Immunology, University of Rochester, Rochester, NY, United States, <sup>3</sup>Department of Biomedical Engineering, University of Rochester, Rochester, NY, United States, <sup>4</sup>Albany College of Pharmacy and Health Sciences, Albany, NY, United States, <sup>5</sup>Department of Physics and Astronomy, University of Rochester, Rochester, NY, United States, <sup>6</sup>Department of Electrical and Computer Engineering, University of Rochester, Rochester, NY, United States, <sup>7</sup>Clinical and Translational Science Institute, University of Rochester, Rochester, NY, United States, <sup>8</sup>Department of Biostatistics and Computational Biology, University of Rochester, Rochester, NY, United States, <sup>9</sup>Department of Imaging Sciences, University of Rochester, Rochester, NY, United States, <sup>10</sup>Department of Neuroscience, University of Rochester, Rochester, NY, United States

**Introduction:** Due to advances in combined anti-retroviral treatment (cART), there is an increased burden of age-related cerebrovascular disease (CBVD), in people living with HIV (PWH). The underlying CNS injury can be assessed by measuring cerebral blood flow (CBF) and cerebrovascular reactivity (CVR).

**Methods:** 35 treatment-naïve PWH and 53 HIV negative controls (HC) were enrolled in this study. Study participants underwent T1-weighted anatomical, pseudo-continuous arterial spin labeling, and resting-state functional MRI to obtain measures of CBF and CVR prior to starting cART treatment and at two-time points (12 weeks and 2 years) post-cART initiation. Controls were scanned at the baseline and 2-year visits. We also measured plasma levels of microparticles of endothelial and glial origin and well-known endothelial inflammation markers, ICAM-1 and VCAM-1, to assess HIV-associated endothelial inflammation and the interaction of these peripheral markers with brain neurovascular function.

**Results:** HIV infection was found to be associated with reduced CVR and increased levels of endothelial and glial microparticles (MPs) prior to initiation of cART. Further, CVR correlated negatively with peripheral MP levels in PWH.

**Discussion:** Our results suggest that while cART treatment has a beneficial effect on the neurovascular function after initiation, these benefits are suboptimal over time.

## KEYWORDS

HIV, cART, neuroinflammation, neuroimaging, cerebral vascular reactivity, cerebral blood flow, resting-state fMRI, microparticles

## 1. Introduction

Combination antiretroviral therapy (cART) has dramatically changed the outlook of infection with Human Immunodeficiency Virus, type 1 (HIV), from one with no treatment to that of a manageable chronic disease, and people with HIV (PWH) now have a lifespan getting closer to those uninfected albeit with a larger burden of comorbidities, including vascular disease (1). Cerebrovascular disease (CBVD) is associated with aging and is more frequent among PWH (2). It poses a significant disease burden in this vulnerable population, especially as nearly half of PWH in USA are age 50 and older. CBVD is a leading cause of vascular cognitive impairment and dementia that may further contribute to HIV-associated cognitive impairment (3–7).

HIV is a neurotropic virus and is known to enter the central nervous system (CNS) as early as 8 days post infection (8). Of interest, HIV can also infect pericytes, a key cellular component of the blood–brain barrier (BBB) (9). Systemic chronic inflammation associated with HIV infection may also contribute to BBB permeability (10). Similarly, cART effect on endothelial cell may facilitate BBB disruption (11). The aging HIV population also faces traditional risk factors, including diabetes, dyslipidemia, and cardiovascular disease, that can contribute to CBVD. Large epidemiological studies suggest that CBVD is more common in PWH compared to HIV uninfected individuals and is considered a major driver of CNS injury (3–7).

Advanced neuroimaging techniques such as arterial spin labeling (ASL) and resting-state functional magnetic resonance imaging (rs-fMRI) allow non-invasive assessment of cerebral blood flow (CBF) and cerebrovascular reactivity (CVR), respectively (12–17). CBF is a measure of brain perfusion and can be used to assess both local changes in perfusion pressure and redistribution of blood flow within that region's vascular network. CBF is tightly coupled to neuronal function, though several components of the functional neurovascular unit (neurons, astrocytes, endothelial, and pericytes) contribute to overall CBF regulation (18). CVR reflects a compensatory change in cerebral arteries in response to a vasoactive stimulus such as CO<sub>2</sub> to meet the changing blood supply demands of the CNS (13). Since decreased CVR is associated with CBVD, CVR mapping can be used as an imaging marker to assess cerebral vascular territories with or at risk of CBVD (19). There are a few reports that have investigated CBF in PWH. Ances et al. (20) have shown reduced resting CBF in the basal ganglia and visual cortex of PWH compared to HIV negative healthy controls (HC). CBF abnormalities have also been documented in PWH with cognitive impairment (20–22). However, rs-fMRI based CVR without CO<sub>2</sub> challenge (15, 16) is a relatively newer measure of CNS neurovascular function, especially in the context of HIV infection.

In addition to these neuroimaging vascular markers, plasma levels of microparticles (MPs) of endothelial and glial origin can be informative of BBB alteration. Endothelial cells (ECs) lining the inner walls of cerebral blood vessels are critical for maintenance of neurovascular homeostasis, and injury to these cells can affect many critical functions, including CBF, CVR, and BBB function. In addition, damage to endothelial cells as well as their activation can result in release of MPs by the ECs and also leakage of glial MPs into the periphery.

Microparticles are small membrane-bound micro-vesicles of 0.1–1 μm in diameter (23, 24). They act as signaling shuttles that

can deliver the intracellular cargo from the cell of their origin to the recipient cell and can contribute to inflammation in various chronic conditions, including HIV infection and vascular disease, as shown by our group (25) and others (26–35). Circulating microparticles of glial origin (expressing GFAP-Glial Fibrillary acidic protein) have been considered a marker of neurovascular injury during HIV infection and other CNS disorders (36–40). Further, our group (41, 42) and others (43, 44) have shown that sonic hedgehog (Shh+) signaling during astrocyte–endothelial communication is neuroprotective and is found to be disrupted during HIV infection and can lead to increased BBB permeability. These studies indicate that MPs of glia and endothelial origins could be used as biomarkers of BBB injury. However, it is not known how these peripheral markers correlate with neurovascular neuroimaging markers.

In order to examine the effect of cART on the neurovascular function, we examined longitudinal changes in CVR, CBF, and MPs of astrocytic and endothelial origin in PWH before and after initiation of cART.

## 2. Materials and methods

This study was reviewed and approved by the Research Subjects Review Board at the University of Rochester, and all study participants signed a written informed consent prior to undergoing study procedures. Details of the study cohort have been previously reported (45). For the analyses reported here, data on 88 unique study participants, 35 (32 male) treatment-naïve PWH and 53 (27 male) age-matched HIV– healthy controls were available at baseline. However, the total number of study participants in the HIV+ cohort decreased from 35 to 32 at 12 weeks and further declined to 15 at year 2. Similarly, the total number of study participants in HIV– cohort went from 53 at baseline visit to 25 at year 2 visit. After initiation of cART the mean CD4 counts were 580 cells/μl (SD: 261) at week 12 and 848 cells/μl (SD: 271) at year 2. Similarly mean viral load was 513 copies/mL (*n* = 8, SD: 2629) at week 12 and 20 copies/mL (*n* = 10, SD: 42) at year 2. In rest of the study participants, viral loads were below detectable limit. Demographic and clinical characteristics of study participants are presented in Table 1.

All participants underwent a comprehensive clinical, laboratory, and neuroimaging evaluation. PWH were assessed at baseline (BSL, prior to initiation of cART) and 12 weeks (W12), and 2 years (Y2) post-cART initiation, while healthy controls were assessed at BSL, and YR 2 only. All PWH were antiretroviral treatment-naïve prior to enrollment and met the following laboratory parameters within 30 days of baseline evaluation: hemoglobin  $\geq 9.0$  g/dL, serum creatinine  $\leq 2 \times$  ULN, AST (SGOT), ALT (SGPT), and alkaline phosphatase  $\leq 2 \times$  upper limit of normal. Participants with severe pre-morbid or comorbid psychiatric disorders, such as diagnoses of schizophrenia, bipolar disorder, and active depression, were excluded. Additional exclusionary criteria were stroke, head trauma resulting in the loss of consciousness for more than 30 min, multiple sclerosis, brain infections (except for HIV-1), space-occupying brain lesions requiring acute or chronic therapy, dementia as established by the HAND definition, active alcohol and drug abuse within 6 months of study entry, and conditions preventing MRI scanning (claustrophobia and metallic implants). Study participants meeting criteria for HIV-associated mild neurocognitive disorder (MND) or HIV-associated

TABLE 1 Demographic characteristics of study participants at baseline visit.

Characteristics	HIV+ (N = 35)	HIV- (N = 53)	p-value
Age, mean (SE)	34.2 (2.2)	36.9 (1.6)	0.329
<b>Gender, n (%)</b>			
Female	3 (8.6%)	26 (49.1%)	<0.001
Male	32 (91.4%)	27 (50.9%)	
<b>Ethnicity, n (%)</b>			
Hispanic or Latino	3 (8.6%)	2 (3.8%)	0.383
Not Hispanic or Latino	32 (91.4%)	51 (96.2%)	
<b>Race, n (%)</b>			
Caucasian	17 (48.6%)	43 (81.1%)	<0.001
Black.AA	18 (51.4%)	5 (9.4%)	
Other	0 (0%)	4 (7.5%)	
Missing	0 (0%)	1 (1.9%)	
<b>Diabetes type II, n (%)</b>			
True	1 (2.9%)	1 (1.9%)	-
FALSE	34 (97.1%)	48 (90.6%)	
Missing	0 (0%)	4 (7.5%)	
<b>High blood pressure, n (%)</b>			
True	3 (8.6%)	4 (7.5%)	-
FALSE	32 (91.4%)	45 (84.9%)	
Missing	0 (0%)	4 (7.5%)	
<b>Current smoker</b>			
True	16 (45.7%)	5 (9.4%)	<0.001
FALSE	19 (54.3%)	48 (90.6%)	
<b>Education, n (%)</b>			
Less than or equal to 12 years	11(31.4%)	6(11.3%)	0.027
More than 12 years	24(68.6%)	47(88.7%)	
<b>Previous smoker</b>			
True	9 (25.7%)	14 (26.4%)	-
FALSE	26 (74.3%)	39 (73.6%)	
<b>CD4, mean (SD), cells/uL</b>			
Baseline	496 (261)	-	-
CD4 Nadir	482.3 (42.7)	-	-
<b>Viral load, mean (SD), copies/mL</b>			
Baseline	90,872 (142,938)	-	-
Week 12, undetectable in n=8	513 (2,629)	-	-
Year 2, undetectable in n=10	20 (42)	-	-

p-values are obtained by either two-group Welch's unequal variances *t*-test (for continuous variables) or Fisher exact test (for categorical variables). PWH, people with HIV; HC, HIV negative healthy controls; SE, standard error.

asymptomatic neurocognitive impairment (ANI) were eligible to participate. Exclusion criteria for healthy controls differ only for HIV status.

## 2.1. MRI acquisition and analysis

MRI was performed on a 3 T Siemens TIM Trio scanner (Erlangen, Germany) equipped with a 32-channel head coil at the University of Rochester's Center for Advanced Brain Imaging and Neurophysiology (UR CABIN). A T1-weighted (T1w) 3D magnetization-prepared rapid acquisition gradient echo (MPRAGE) images were acquired with the scan parameters: inversion time (TI) = 1,100 ms, repetition time (TR)/echo time (TE) = 2,530 ms/2.33 ms, resolution = 1.0 × 1.0 × 1.0 mm<sup>3</sup>. Resting-state fMRI scans were acquired using a gradient echo-echo planar imaging (GE-EPI) sequence (TR/TE = 2,000 ms /30 ms, 150 volumes, resolution = 4.0 × 4.0 × 4.0 mm<sup>3</sup>). Participants were instructed to keep their eyes closed for the duration of the sequence. Perfusion imaging was performed using a pseudo continuous arterial spin labeling (pcASL) sequence (TR/TE = 3,530/22.62 ms, resolution = 3.8 × 3.8 × 5 mm<sup>3</sup>) using a tag-control pair technique with 36 averages with a 1.5 s labeling duration and 1.5 s single post label delay (PLD). The equilibrium magnetization of arterial blood image (M<sub>0</sub>) was acquired with one average at a TR = 5,000 ms.

T1w images were reoriented to standard orientation, cropped, bias-field corrected, skull-stripped, linearly and nonlinearly registered to MNI152-2 mm standard space, and segmented by tissue type using FSL's (FMRIB's Software Library, version 5.11) anatomical processing script (fsl\_anat) (46, 47). Structural images were used for co-registration of the functional and perfusion images to anatomical and standard spaces. Tissue maps were used to account for partial volume effects in functional processing. Regions of interests (ROIs) were determined *a priori* and extracted using the Harvard-Oxford cortical and subcortical atlases available in FSL. Each ROI was warped from standard to native spaces and binarized before being applied as a mask against each imaging metric map. The mean and standard deviation of each metric were calculated using FSL's fslstats tool within each ROI. ROIs included in these analyses were the Amygdala (Amyg), Caudate Nucleus (CN), Globus Pallidus (GP), Hippocampus (Hippo), Putamen (PUT), Thalamus (TH), Precuneus Cortex (PreC), global white matter (GWM), and global gray matter (GGM). Bilateral ROIs were merged prior to calculating metric means.

The rs-fMRI data processing was carried out using FEAT (fMRI Expert Analysis Tool) Version 6.00, part of FSL (47). Registration to high-resolution structural and/or standard space images was carried out using FLIRT (48). Registration from high-resolution structural to standard space was then further refined using FNIRT nonlinear registration (49). The following pre-statistics processing was applied: motion correction using MCFLIRT (48), non-brain removal using BET (50), spatial smoothing using a Gaussian kernel of FWHM 5 mm, grand-mean intensity normalization of the entire 4D dataset by a single multiplicative factor, and high-pass temporal filtering (Gaussian-weighted least-squares straight line fitting, with sigma = 50.0 s).

CVR maps were estimated with the global signal regression coefficient method using rs-fMRI BOLD images (15), providing qualitative reactivity indices for each subject at each study visit. Briefly, the preprocessing steps encompassed motion correction, spatial smoothing through a Gaussian filter with a full-width-half-maximum (FWHM) of 4 mm, and a linear detrending. Subsequently, building upon previous findings in healthy controls that attributed global

resting state BOLD fluctuations primarily to natural variations in ETCO<sub>2</sub> levels within the frequency range of 0.02 to 0.04 Hz, we applied a band-pass filter to temporarily filter the rs-BOLD data within this specific frequency range. The gray matter tissue segmentation was then used as a mask for calculating the global average gray matter rs-fMRI signal to be used as a regressor against voxel-wise BOLD signals. The global signal has been previously shown to act as a surrogate for respiratory and cardiac fluctuations (15). The global-average gray matter rs-fMRI signal was regressed against the preprocessed BOLD signal at each voxel, where the slope of the regression was taken as a CVR index. Normalization of this index by the whole-brain average provides a qualitative estimate of CVR.

ASL images were processed with the Oxford ASL tool (51). Preprocessing included motion correction using MCFLIRT, slice-timing correction, distortion correction, spatial regularization, partial volume correction, and registration to high-resolution anatomical space using the boundary-based registration (BBR) algorithm and to 2 mm MNI-152 standard space using FNIRT nonlinear registration (52). CBF quantification was run in three steps: Bayesian inference for CBF according to the Buxton kinetic curve model, Bayesian inference of further parameters as applicable to single-post label delay data, and Bayesian inferences with spatial prior to fine tune the model parameters, initialized by the high-resolution anatomical image (53, 54).

## 2.2. Blood biomarkers

Plasma was isolated from whole blood samples from study participants by centrifugation and was cryopreserved. Plasma levels of astrocytic microparticles were determined by the expression of glial fibrillary acidic protein (GFAP) and sonic hedgehog (Shh). Endothelial-derived microparticles were assessed via expression of CD144 and CD62L. Measurements were performed by volumetric flow cytometry analysis using Accuri C6 (BD Biosciences, San Jose CA, United States) as described previously (25). Plasma levels of soluble Intracellular adhesion molecule 1 (ICAM-1) and vascular cell adhesion molecule 1 (VCAM-1) were measured by DuoSET ELISA kits from R and D systems as per manufacturer's instructions.

## 2.3. Statistical analysis

Comparisons between two independent groups (e.g., PWH vs. control study participants at baseline) were conducted by either the two-group Welch's unequal variances *t*-test (for continuous variables) or Fisher exact test (for categorical variables). Paired *t*-tests were used to compare the levels of continuous variables in PWH study participants between time points baseline, 12 week, and year two visits. A value of  $p < 0.05$  was considered statistically significant for a single hypothesis testing problem. In the subset of subjects with blood biomarkers, we examined the relationships between these markers and regional CVR and CBF metrics. We performed the Spearman Correlation Test between the blood markers and regional imaging metrics at each study visit. The Benjamini-Hochberg multiple testing procedure was utilized to regulate the false discovery rate (FDR) at a significant level of 0.05. All statistical analyses were performed in R 3.6.2 (R Foundation for Statistical Computing, Vienna, Austria) and

GraphPad Prism (version 9.0, GraphPad Software, Inc., San Diego, CA).

## 3. Results

### 3.1. HIV, cART, and neuroimaging markers

Figure 1 presents CVR and CBF maps from a study participant with HIV infection. Among all the different ROIs measured, only CN, TH, GWM, and GGM exhibited statistically significant differences between groups; hence, results pertaining to only these three ROIs are discussed. Univariate analysis showed that at baseline, CVR was significantly lower in CN ( $p=0.015$ ), TH ( $p=0.022$ ), GWM ( $p=0.018$ ) and GGM ( $p=0.02$ ) in PWH as compared to HIV uninfected controls (Figures 2A–D). During longitudinal follow-up, at 2 years, in HIV–controls, CVR values remain unchanged. In PWH, after initiation of cART, there was a moderate increase in CVR in all three regions (statistically significant only in GWM,  $p=0.042$ ) at 12 weeks post-treatment, suggesting a beneficial effect of the treatment. At 2 years post-treatment, however, CVR values show a decreasing trend, albeit not to the same levels as at baseline, with statistical significance only in GGM ( $p=0.02$ , Figure 2D). Univariate analysis showed no difference in CBF (measured as mL/100 grams of brain tissue/min) at baseline between PWH and control groups (Figures 2E–H). Similar to CVR, CBF remains almost unchanged in longitudinal follow-up in healthy controls. In PWH there was an increase in CBF at week 12 (statistically significant in GWM,  $p=0.039$  and TH,  $p=0.01$ ), followed by a decline at 2 years of follow-up (statistically significant in GWM,

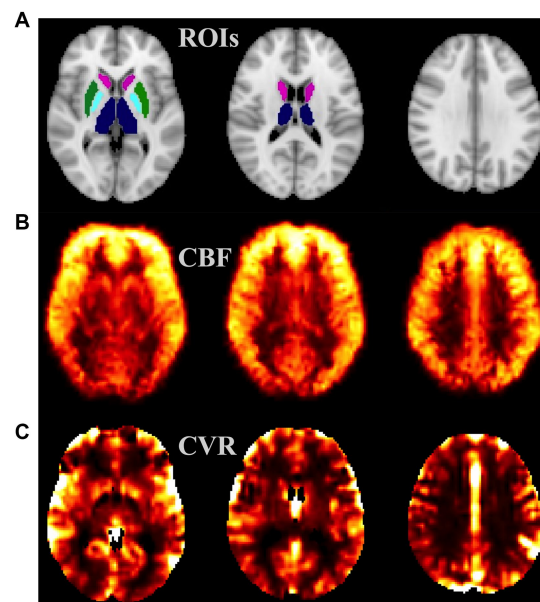
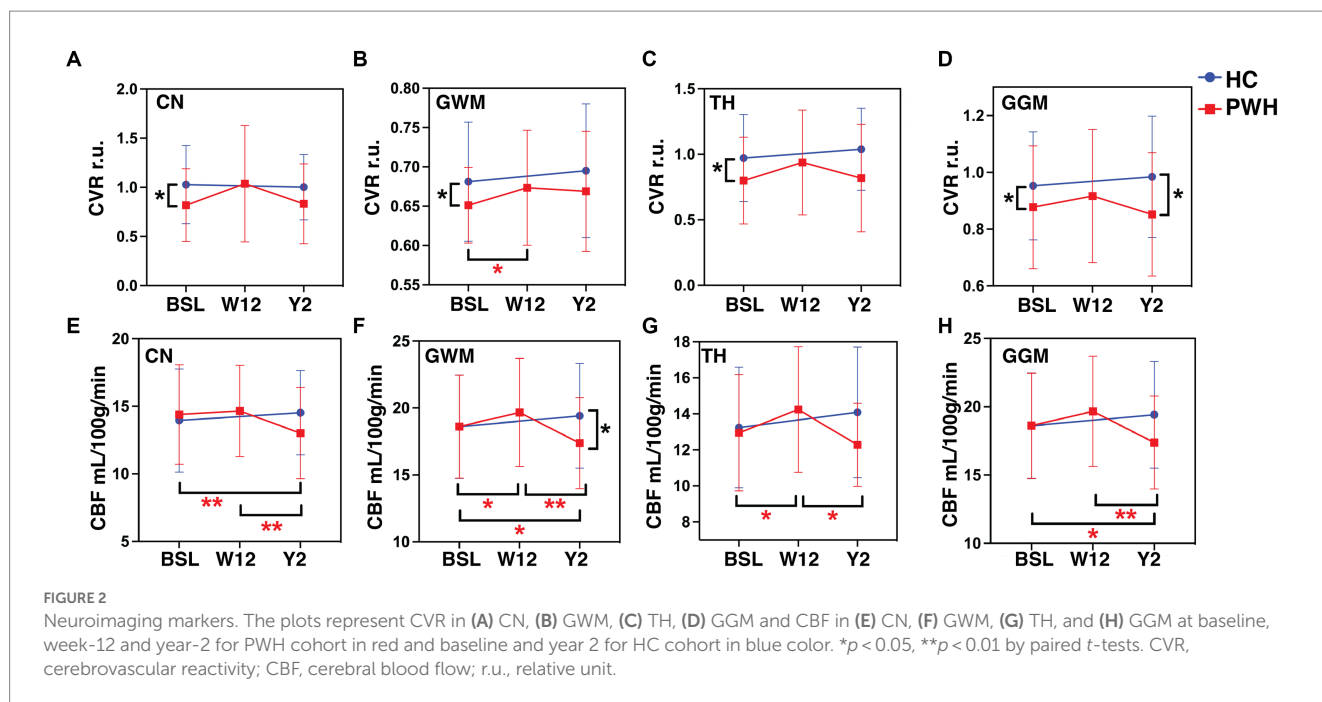


**FIGURE 1**  
Example MRI maps from a healthy subject: (A) ROIs considered—TH (blue), CN (magenta), PUT (green), and GP (cyan); (B) cerebral blood flow (CBF) map, intensity scale: 0–50 mL/100 g/min; (C) cerebrovascular reactivity (CVR) map, intensity scale: 0–3 relative unit. CN, caudate nucleus; PUT, putamen; GP, Globus Pallidus; ROI, region of interest.



$p=0.017$  and GGM,  $p=0.023$ , as compared to baseline visit). Interestingly, there was a significant decline in CBF at year 2 as compared to week 12 time point in all four ROIs, CN, GWM, TH, and GGM ( $p=0.0017$ ,  $0.0024$ ,  $0.0122$ , and  $0.0018$ , respectively). This trend is similar to what we observed for CVR.

### 3.2. HIV, cART, and blood biomarkers

Univariate analysis did not show any significant difference in plasma levels of ICAM-1 between the two groups at any time point. There was a trend toward increase in ICAM-1 levels within both the groups, at each successive visit but the difference was not statistically significant (Figure 3A).

With respect to VCAM, at baseline, HIV uninfected group had higher plasma levels compared to PWH (Figure 3B;  $p=0.0427$ ). This difference did not persist at the 2-year follow-up. In addition to these well-known markers of endothelial activation, we also measured microparticles of endothelial (CD144+ MPs, CD144+CD62L+ MPs) and glial (GFAP+ MPs, GFAP+Shh+ MPs) origin. With the exception of CD144+CD62L+ MPs, all other types showed significantly higher levels in PWH compared to controls at baseline (Figures 3C–F;  $p=0.016$ ,  $0.0239$ ,  $0.0092$ , respectively). The differences between the two groups were not statistically different after 2 years of cART treatment. Within the PWH group, the largest treatment effect was observed in GFAP+ MPs and GFAP+Shh+ MPs.

### 3.3. Correlations between neuroimaging and blood biomarkers

At the baseline visit, CVR in CN showed significantly negative correlations with CD144+ MPs ( $r: -0.4371$ ,  $p=0.01$ ), CD144+CD62L+ MPs ( $r: -0.4142$ ,  $p=0.0155$ ) and GFAP+Shh+ MPs ( $r: -0.4117$ ,  $p=0.016$ ) only in PWH (Figures 4A–C, respectively). While there

were no correlations at the week 12 visit, GFAP+Shh+ MPs were again significantly negatively correlated with CVR in CN at year 2 in PWH (Figure 4D,  $r: -0.5989$ ,  $p=0.034$ ). CVR in any regions did not correlate with any blood markers in controls at any time point (data not shown).

In the case of CBF, at baseline, the only significant negative correlations were between CD144+CD62L MPs and CBF in GWM (Figure 5A;  $r: -0.3336$ ,  $p=0.05$ ) and CBF in TH (Figure 5B;  $r: -0.3876$ ,  $p=0.0226$ ) in the PWH. Interestingly, at week 12, all four types of MPs (CD144+, CD144+CD62L+, GFAP+ and GFAP+Shh+) correlated positively with CBF in CN (Figures 5C–F;  $r: 0.4347$ ,  $p=0.013$ ;  $r: 0.4197$ ,  $p=0.0175$ ;  $r: 0.4846$ ,  $p=0.0052$ ;  $r: 0.3896$ ,  $p=0.0285$ , respectively) but there were no correlations at year 2 (data not shown). Similar to CVR, controls did not show any correlations between CBF and blood biomarkers.

## 4. Discussion

The results from this study suggest that CVR, endothelial, and glia MPs are early markers of neurovascular dysfunction in cART naïve PWH. Most of these markers improved shortly after cART treatment; however, the beneficial effect of cART treatment diminished over time. Abnormalities in CVR were found in both subcortical gray matter regions (CN and TH) and white global white matter (GWM), indicating a diffuse involvement of the brain microcirculation. The trend of decreased CVR during chronic cART-treated PWH was associated with a decrease in CBF, especially in the GWM.

Two recent studies have also assessed CVR in PWH using alternative approaches to ours. Callen et al. (55) used changes in CBF induced by intravenous acetazolamide and found decreased CVR in the frontal lobe and basal ganglia. Chow et al. (56) used transcranial Doppler ultrasound (TCD) and breath-holding to assess mean flow velocity changes to infer CVR. Higher CVR was associated with a higher score on the Montreal Cognitive Assessment.

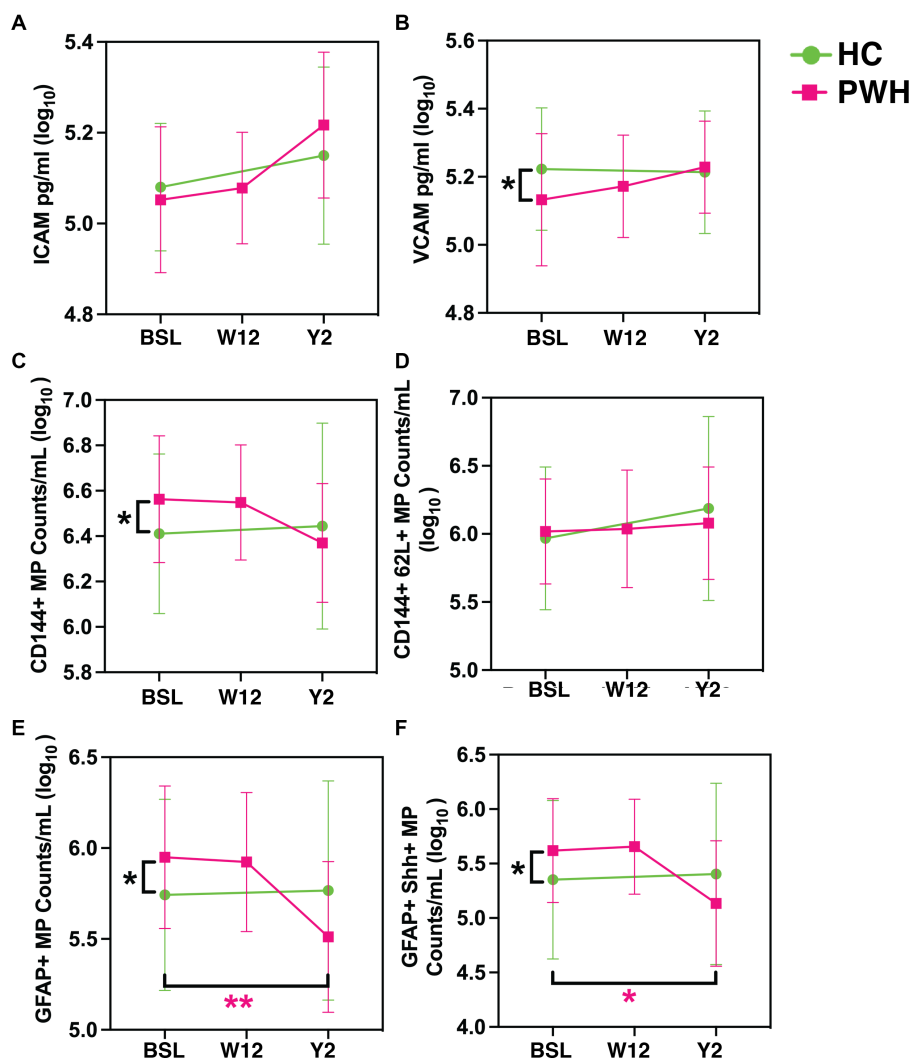


**FIGURE 3** Blood biomarkers. The plots represent plasma levels of (A) ICAM-1, (B) VCAM-1, (C) CD144+ endothelial MPs, (D) CD144+CD62L+ endothelial MPs, (E) GFAP+ astrocytic MPs, and (F) GFAP+Shh+ astrocytic MPs at baseline, week-12 and year-2 for HIV+ cohort in red and baseline and year 2 for HIV- cohort in green. \* $p < 0.05$ , \*\* $p < 0.01$ , \*\*\* $p < 0.001$  by paired t-tests. MPs, microparticles.

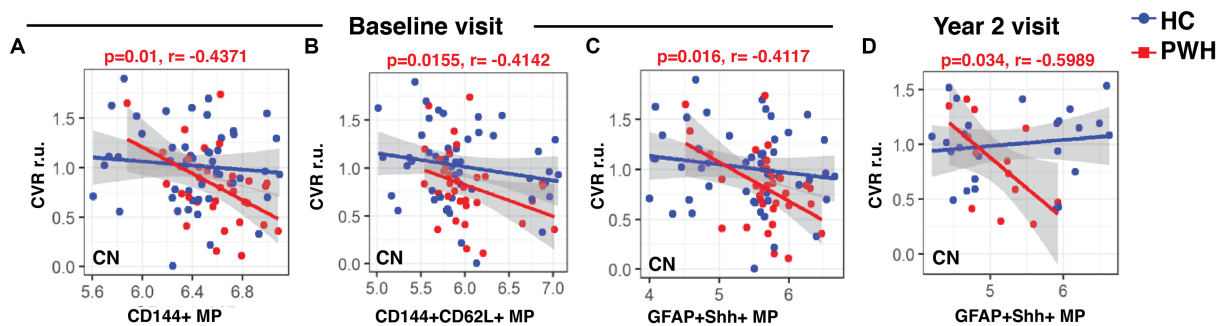


**FIGURE 4** Associations between CVR and blood biomarkers. The linear regression plots show CVR in CN at baseline in PWH cohort showed significant negative correlations with (A) CD144+ and (B) CD144+CD62L+ endothelial MPs and also with (C) GFAP+Shh+ astrocytic MPs. (D) CVR at year-2 continued to show strong negative correlations with CVR in PWH cohort. CVR, cerebrovascular reactivity; r.u., relative unit.

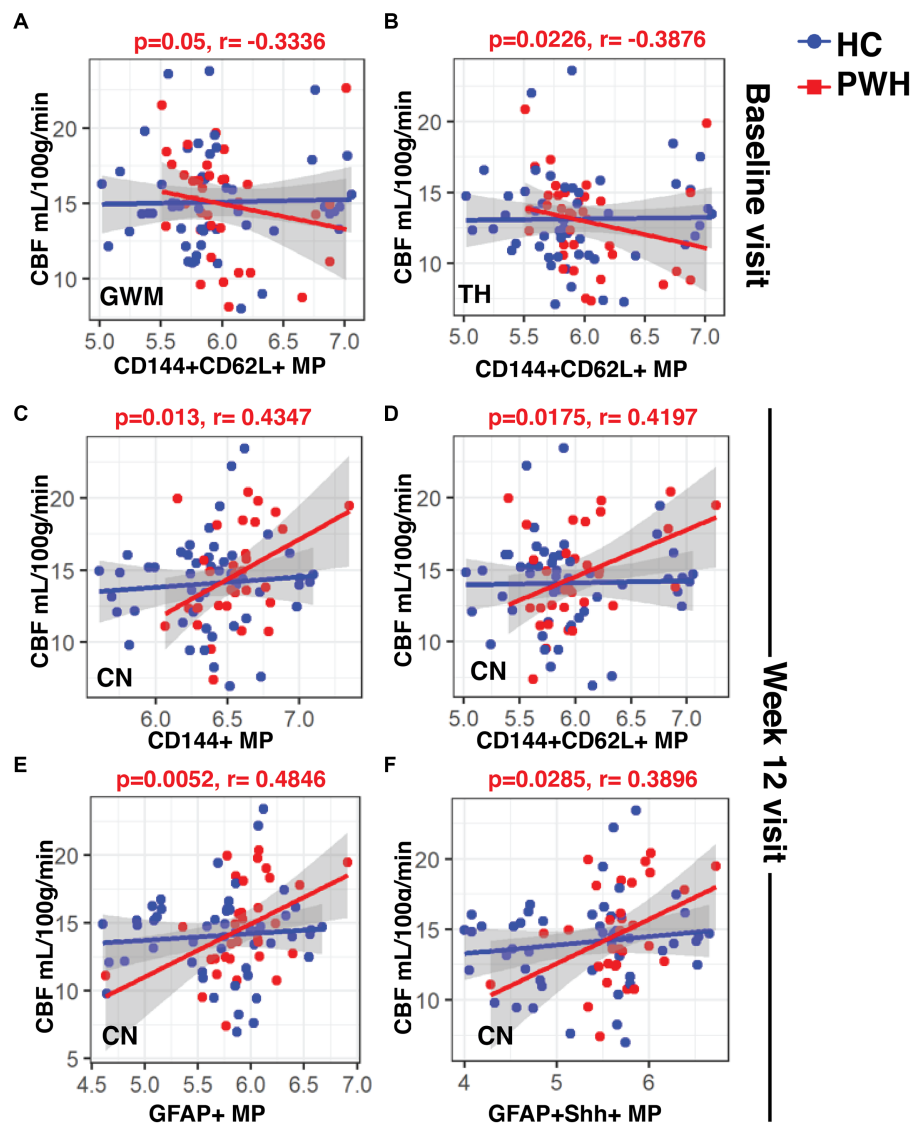


FIGURE 5

Associations between CBF and blood biomarkers. The linear regression plots show (A) CBF in GWM and (B) TH at baseline in PWH cohort showed significant negative correlations with CD144+CD62L+ endothelial MPs. (C–F) CBF CN in PWH cohort at week-12 correlated positively with all types of MPs. CBF, cerebral blood flow; MPs, microparticles.

Since the cohort of PWH we enrolled was relatively young (average age 34 years) with preserved immune function before starting cART (average nadir and baseline CD4+ cell count > 400 cell/uL), it could be envisioned that PWH as they age would be further exposed to CBVD and in particular to cerebral small vessel disease (CSVD). CVR is closely linked to the regulation of the microcirculation, thus, is reduced in CSVD (57). Consistent with these implications are recent studies showing a higher prevalence of CSVD in PWH compared to HC (2, 58).

CBF in our study did not differ between PWH cART naïve prior to starting treatment and controls, suggesting that more significant alteration in tissue perfusion is necessary before changes in CBF can be captured. In contrast, CVR is more closely related to CSVD (59).

CVR is a marker of endothelial function; therefore, we assessed the relationship between CVR and plasma levels of endothelial-derived MPs. We measured MPs that expressed endothelial marker CD144 (CD144+ MPs) and also MPs double positive for CD144 and

CD62L (aka L-selectin), which is a marker of endothelial activation (CD144+CD62L+ MPs). Endothelial markers, including ICAM-1 and VCAM-1 were also measured. The increased plasma levels of CD144+ MPs in PWH compared to controls are consistent with the expected effect of inflammation before cART initiation and the subsequent decline with reduced inflammation during cART. In contrast, VCAM-1 level before cART were surprisingly lower in PWH and normalized with treatment. This finding needs to be confirmed in further investigations. On the other hand, ICAM-1 did not differ between groups.

Systemic inflammation associated with HIV infection could also lead to an altered BBB. In this study, we observed that GFAP+ MPs were elevated in cART naïve PWH, suggesting an increased BBB permeability. The beneficial response to cART treatment continued during the two-year follow-up. We next examined the temporal correlation between CVR and blood biomarkers. CVR in CN correlated negatively with endothelial and glial MP levels at baseline study visit, only in PWH. At year-2, despite a

smaller number of study participants, glial MPs continue to show an even stronger negative correlation with CVR in caudate. Endothelial MPs also correlated negatively with CBF in GWM and Thalamus at baseline visit in PWH. However, after cART both MPs and CBF decreased, making now their relationship positively correlated but likely not causally related. From these results, CVR and endothelial and glia MPs provide a consistent mechanistic relationship when assessing cerebral microcirculation. When assessing CVR directly is not possible, for example in resource-limited settings where MRI facilities are not readily available, these blood biomarkers could be more easily implemented.

Our study has a few limitations. First, the sample size of our study is small due to both enrollment restrictions/difficulties with a cART-naïve population and a high attrition rate. Second, as the study recruited study participants that were treatment-naïve to cART, a young study population limited the evaluation of the effects of cART in older PWH. Also, PWH in this geographical location are heavily skewed toward male sex-at-birth. Owing to that, we were able to enroll only three cART naïve female study participants and thus were not able to evaluate the effect of sex. Furthermore, the calculation of CVR from resting-state fMRI has limitations as well. While methods have been developed to qualitatively assess a relative CVR index based on resting-state data (15, 16), the gold standard to quantify and assess CVR is using a vasoactive stimulus task-based breathing challenge (60). An additional limitation is the post label delay (PLD) of 1.5 s used in ASL, shorter than the 1.8 s currently recommended (61). It should be noted that our protocol was implemented prior to this recommendation. However, the relative young age of the cohort enrolled likely minimizes the impact of the shorter PLD. Despite these caveats, our study design allows for a unique approach to study and separate the effects of acute and chronic HIV infection and cART treatment on brain cerebrovascular function.

## 5. Conclusion

To the best of our knowledge, this is the only study that specifically investigates longitudinal changes in CVR, CBF, endothelial, and glia MPs before and after cART initiation. Our findings indicate that untreated HIV infection, even with relatively preserved immune function, affects brain microcirculation. While cART normalizes endothelial and glia MPs levels, effects on CVR and CBF seem less effective over time, possibly predisposing PWH to CSVD.

## Data availability statement

The original contributions presented in the study are included in the article/supplementary material, further inquiries can be directed to the corresponding author.

## References

- Marcus JL, Leyden WA, Alexeeff SE, Anderson AN, Hechter RC, Hu H, et al. Comparison of overall and comorbidity-free life expectancy between insured adults with and without HIV infection, 2000–2016. *JAMA Netw Open*. (2020) 3:e207954. doi: 10.1001/jamanetworkopen.2020.7954
- Murray KD, Uddin MN, Tivarus ME, Sahin B, Wang HZ, Singh MV, et al. Increased risk for cerebral small vessel disease is associated with quantitative susceptibility mapping in HIV infected and uninfected individuals. *Neuroimage Clin*. (2021) 32:102786. doi: 10.1016/j.nicl.2021.102786
- Sico JJ, Chang CC, So-Armah K, Justice AC, Hylek E, Skanderson M, et al. HIV status and the risk of ischemic stroke among men. *Neurology*. (2015) 84:1933–40. doi: 10.1212/WNL.0000000000001560
- Marcus JL, Leyden WA, Chao CR, Chow FC, Horberg MA, Hurley LB, et al. HIV infection and incidence of ischemic stroke. *AIDS*. (2014) 28:1911–9. doi: 10.1097/QAD.0000000000000352
- Vinikoor MJ, Napravnik S, Floris-Moore M, Wilson S, Huang DY, Eron JJ. Incidence and clinical features of cerebrovascular disease among HIV-infected adults in the

## Ethics statement

The studies involving humans were approved by University of Rochester Research Subject Review Board. The studies were conducted in accordance with the local legislation and institutional requirements. The participants provided their written informed consent to participate in this study.

## Author contributions

MS and MU: study design, conducting experiments, acquiring data, analyzing data, and writing the manuscript. VS, AP, and YZ: conducting experiments, acquiring data, and analyzing data. KM: conducting experiments, acquiring data, analyzing data, and writing the manuscript. AT: data entry and database management. LW: statistical support. MT and JZ: manuscript review for intellectual content. XQ: statistical support and manuscript review for intellectual content. GS: study design, funding acquisition, and manuscript writing and review for intellectual content. All authors contributed to the article and approved the submitted version.

## Funding

This work was supported by the National Institutes of Health, grant numbers R01MH099921 and R01AG054328.

## Acknowledgments

The authors would like to thank the participants, study coordinators, and data management team.

## Conflict of interest

The authors declare that the research was conducted in the absence of any commercial or financial relationships that could be construed as a potential conflict of interest.

## Publisher's note

All claims expressed in this article are solely those of the authors and do not necessarily represent those of their affiliated organizations, or those of the publisher, the editors and the reviewers. Any product that may be evaluated in this article, or claim that may be made by its manufacturer, is not guaranteed or endorsed by the publisher.

- southeastern United States. *AIDS Res Hum Retrovir.* (2013) 29:1068–74. doi: 10.1089/aid.2012.0334
6. Mateen FJ, Post WS, Sacktor N, Abraham AG, Becker JT, Smith BR, et al. Long-term predictive value of the Framingham risk score for stroke in HIV-positive vs HIV-negative men. *Neurology.* (2013) 81:2094–102. doi: 10.1212/01.wnl.0000437296.97946.73
7. Chow FC, Regan S, Feske S, Meigs JB, Grinspoon SK, Triant VA. Comparison of ischemic stroke incidence in HIV-infected and non-HIV-infected patients in a US health care system. *J Acquir Immune Defic Syndr.* (2012) 60:351–8. doi: 10.1097/QAI.0b013e31825c7f24
8. Valcour V, Chalermchai T, Sailasuta N, Marovich M, Lerdlum S, Suttichom D, et al. Central nervous system viral invasion and inflammation during acute HIV infection. *J Infect Dis.* (2012) 206:275–82. doi: 10.1093/infdis/jis326
9. Bertrand L, Cho HJ, Toborek M. Blood-brain barrier pericytes as a target for HIV-1 infection. *Brain.* (2019) 142:502–11. doi: 10.1093/brain/awy339
10. Rahimy E, Li FY, Hagberg L, Fuchs D, Robertson K, Meyerhoff DJ, et al. Blood-brain barrier disruption is initiated during primary HIV infection and not rapidly altered by antiretroviral therapy. *J Infect Dis.* (2017) 215:1132–40. doi: 10.1093/infdis/jix013
11. Kline ER, Sutliff RL. The roles of HIV-1 proteins and antiretroviral drug therapy in HIV-1-associated endothelial dysfunction. *J Investig Med.* (2008) 56:752–69. doi: 10.1097/JIM.0b013e3181788d15
12. Wierenga CE, Hays CC, Zlatar ZZ. Cerebral blood flow measured by arterial spin labeling MRI as a preclinical marker of Alzheimer's disease. *J Alzheimers Dis.* (2014) 42:S411–9. doi: 10.3233/JAD-141467
13. Duffin J, Sobczyk O, McKetton L, Crawley A, Poulblanc J, Venkatraghavan L, et al. Cerebrovascular resistance: the basis of cerebrovascular reactivity. *Front Neurosci.* (2018) 12:409. doi: 10.3389/fnins.2018.00409
14. Hoiland RL, Fisher JA, Ainslie PN. Regulation of the cerebral circulation by arterial carbon dioxide. *Compr Physiol.* (2011) 9:1101–54. doi: 10.1002/cphy.c180021
15. Liu P, Li Y, Pinho M, Park DC, Welch BG, Lu H. Cerebrovascular reactivity mapping without gas challenges. *NeuroImage.* (2017) 146:320–6. doi: 10.1016/j.neuroimage.2016.11.054
16. Pinto J, Bright MG, Bulte DP, Figueiredo P. Cerebrovascular reactivity mapping without gas challenges: a methodological guide. *Front Physiol.* (2021) 11:608475. doi: 10.3389/fphys.2020.608475
17. Parkes LM, Rashid W, Chard DT, Tofts PS. Normal cerebral perfusion measurements using arterial spin labeling: reproducibility, stability, and age and gender effects. *Magn Reson Med.* (2004) 51:736–43. doi: 10.1002/mrm.20023
18. Iadecola C. Neurovascular regulation in the normal brain and in Alzheimer's disease. *Nat Rev Neurosci.* (2004) 5:347–60. doi: 10.1038/nrn1387
19. Conijn MM, Hoogduin JM, van der Graaf Y, Hendrikse J, Luijten PR, Geerlings MI. Microbleeds, lacunar infarcts, white matter lesions and cerebrovascular reactivity—a 7 T study. *NeuroImage.* (2012) 59:950–6. doi: 10.1016/j.neuroimage.2011.08.059
20. Ances BM, Sisti D, Vaida F, Liang CL, Leontiev O, Perthen JE, et al. Resting cerebral blood flow: a potential biomarker of the effects of HIV in the brain. *Neurology.* (2009) 73:702–8. doi: 10.1212/WNL.0b013e3181b59a97
21. Chang L, Ernst T, Leonido-Yee M, Speck O. Perfusion MRI detects rCBF abnormalities in early stages of HIV-cognitive motor complex. *Neurology.* (2000) 54:389–96. doi: 10.1212/WNL.54.2.389
22. Ances BM, Roc AC, Wang J, Korczykowski M, Okawa J, Stern J, et al. Caudate blood flow and volume are reduced in HIV+ neurocognitively impaired patients. *Neurology.* (2006) 66:862–6. doi: 10.1212/01.wnl.0000203524.57993.e2
23. Barteneva NS, Fasler-Kan E, Bernimoulin M, Stern JN, Ponomarev ED, Duckett L, et al. Circulating microparticles: square the circle. *BMC Cell Biol.* (2013) 14:23. doi: 10.1186/1471-2121-14-23
24. Marcoux G, Duchez AC, Cloutier N, Provost P, Nigrovic PA, Boilard E. Revealing the diversity of extracellular vesicles using high-dimensional flow cytometry analyses. *Sci Rep.* (2016) 6:35928. doi: 10.1038/srep35928
25. Weber EA, Singh MV, Singh VB, Jackson JW, Ture SK, Suwunnakorn S, et al. Novel mechanism of microvesicle regulation by the antiviral protein Tetherin during HIV infection. *J Am Heart Assoc.* (2020) 9:e015998. doi: 10.1161/JAHA.120.015998
26. Leite AR, Borges-Canha M, Cardoso R, Neves JS, Castro-Ferreira R, Leite-Moreira A. Novel biomarkers for evaluation of endothelial dysfunction. *Angiology.* (2020) 71:397–410. doi: 10.1177/0003319720903586
27. Hijmans JG, Stockelman KA, Garcia V, Levy MV, Brewster LM, Bammert TD, et al. Circulating microparticles are elevated in treated HIV-1 infection and are deleterious to endothelial cell function. *J Am Heart Assoc.* (2019) 8:e011134. doi: 10.1161/JAHA.118.011134
28. Lopez M, San Roman J, Estrada V, Vispo E, Blanco F, Soriano V. Endothelial dysfunction in HIV infection—the role of circulating endothelial cells, microparticles, endothelial progenitor cells and macrophages. *AIDS Rev.* (2012) 14:223–30.
29. da Silva EF, Fonseca FA, Franca CN, Ferreira PR, Izar MC, Salomao R, et al. Imbalance between endothelial progenitor cells and microparticles in HIV-infected patients naive for antiretroviral therapy. *AIDS.* (2011) 25:1595–601. doi: 10.1097/QAD.0b013e32834980f4
30. Simak J, Gelderman MP, Yu H, Wright V, Baird AE. Circulating endothelial microparticles in acute ischemic stroke: a link to severity, lesion volume and outcome. *J Thromb Haemost.* (2006) 4:1296–302. doi: 10.1111/j.1538-7836.2006.01911.x
31. Bernal-Mizrachi L, Jy W, Fierro C, Macdonough R, Velazques HA, Purow J, et al. Endothelial microparticles correlate with high-risk angiographic lesions in acute coronary syndromes. *Int J Cardiol.* (2004) 97:439–46. doi: 10.1016/j.ijcard.2003.10.029
32. Jimenez JJ, Jy W, Mauro LM, Soderland C, Horstman LL, Ahn YS. Endothelial cells release phenotypically and quantitatively distinct microparticles in activation and apoptosis. *Thromb Res.* (2003) 109:175–80. doi: 10.1016/s0049-3848(03)00064-1
33. Preston RA, Jy W, Jimenez JJ, Mauro LM, Horstman LL, Valle M, et al. Effects of severe hypertension on endothelial and platelet microparticles. *Hypertension.* (2003) 41:211–7. doi: 10.1161/01.hyp.0000049760.15764.2d
34. Sabatier F, Darmon P, Hugel B, Combes V, Sanmarco M, Velut JG, et al. Type 1 and type 2 diabetic patients display different patterns of cellular microparticles. *Diabetes.* (2002) 51:2840–5. doi: 10.2337/diabetes.51.9.2840
35. Hosseinzadeh S, Noroozian M, Mortaz E, Mousavizadeh K. Plasma microparticles in Alzheimer's disease: the role of vascular dysfunction. *Metab Brain Dis.* (2018) 33:293–9. doi: 10.1007/s11011-017-0149-3
36. Tian Y, Salsbery B, Wang M, Yuan H, Yang J, Zhao Z, et al. Brain-derived microparticles induce systemic coagulation in a murine model of traumatic brain injury. *Blood.* (2015) 125:2151–9. doi: 10.1182/blood-2014-09-598805
37. Kodidela S, Gerth K, Sinha N, Kumar A, Kumar P, Kumar S. Circulatory astrocyte and neuronal EVs as potential biomarkers of neurological dysfunction in HIV-infected subjects and alcohol/tobacco users. *Diagnostics.* (2020) 10:349. doi: 10.3390/diagnostics10060349
38. Willis CM, Menoret A, Jellison ER, Nicaise AM, Vella AT, Crocker SJ. A refined bead-free method to identify astrocytic exosomes in primary glial cultures and blood plasma. *Front Neurosci.* (2017) 11:335. doi: 10.3389/fnins.2017.00335
39. Schindler SM, Little JP, Klegeris A. Microparticles: a new perspective in central nervous system disorders. *Biomed Res Int.* (2014) 2014:756327. doi: 10.1155/2014/756327
40. Sartori MT, Della Puppa A, Ballin A, Campello E, Radu CM, Saggiorato G, et al. Circulating microparticles of glial origin and tissue factor bearing in high-grade glioma: a potential prothrombotic role. *Thromb Haemost.* (2013) 110:378–85. doi: 10.1160/TH12-12-0957
41. Singh VB, Singh MV, Gorantla S, Poluektova LY, Maggirwar SB. Smoothened agonist reduces human immunodeficiency virus Type-1-induced blood-brain barrier breakdown in humanized mice. *Sci Rep.* (2016) 6:26876. doi: 10.1038/srep26876
42. Singh VB, Singh MV, Piekna-Przybylska D, Gorantla S, Poluektova LY, Maggirwar SB. Sonic hedgehog mimetic prevents leukocyte infiltration into the CNS during acute HIV infection. *Sci Rep.* (2017) 7:9578. doi: 10.1038/s41598-017-10241-0
43. Bohannon DG, Ko A, Filipowicz AR, Kuroda MJ, Kim WK. Dysregulation of sonic hedgehog pathway and pericytes in the brain after lentiviral infection. *J Neuroinflammation.* (2019) 16:86. doi: 10.1186/s12974-019-1463-y
44. Xing G, Zhao T, Zhang X, Li H, Li X, Cui P, et al. Astrocytic sonic hedgehog alleviates intracerebral hemorrhagic brain injury via modulation of blood-brain barrier integrity. *Front Cell Neurosci.* (2020) 14:575690. doi: 10.3389/fncel.2020.575690
45. Weber MT, Finkelstein A, Uddin MN, Reddy EA, Arduino RC, Wang L, et al. Longitudinal effects of combination antiretroviral therapy on cognition and neuroimaging biomarkers in treatment-naive people with HIV. *Neurology.* (2022) 99:e1045–55. doi: 10.1212/wnl.000000000000200829
46. Woolrich MW, Jbabdi S, Patenaude B, Chappell M, Makni S, Behrens T, et al. Bayesian analysis of neuroimaging data in FSL. *NeuroImage.* (2009) 45:S173–86. doi: 10.1016/j.neuroimage.2008.10.055
47. Smith SM, Jenkinson M, Woolrich MW, Beckmann CF, Behrens TE, Johansen-Berg H, et al. Advances in functional and structural MR image analysis and implementation as FSL. *NeuroImage.* (2004) 23:S208–19. doi: 10.1016/j.neuroimage.2004.07.051
48. Jenkinson M, Bannister P, Brady M, Smith S. Improved optimization for the robust and accurate linear registration and motion correction of brain images. *NeuroImage.* (2002) 17:825–41. doi: 10.1016/s1053-8119(02)91132-8
49. Andersson J. M., Smith S. Non-linear registration, aka spatial normalization (FMRIB technical report TR07A2). (2010).
50. Smith SM. Fast robust automated brain extraction. *Hum Brain Mapp.* (2002) 17:143–55. doi: 10.1002/hbm.10062
51. Chappell MAGA, Whitcher B, Woolrich MW. Variational Bayesian inference for a nonlinear forward model. *IEEE Trans Signal Process.* (2009) 57:223–36. doi: 10.1109/TSP.2008.2005752
52. Greve DN, Fischl B. Accurate and robust brain image alignment using boundary-based registration. *NeuroImage.* (2009) 48:63–72. doi: 10.1016/j.neuroimage.2009.06.060
53. Buxton RB, Frank LR, Wong EC, Siewert B, Warach S, Edelman RR. A general kinetic model for quantitative perfusion imaging with arterial spin labeling. *Magn Reson Med.* (1998) 40:383–96. doi: 10.1002/mrm.1910400308
54. Chappell MA, Groves AR, Whitcher B, Woolrich MW. Variational Bayesian inference for a nonlinear forward model. *IEEE Trans Signal Process.* (2008) 57:223–36. doi: 10.1109/TSP.2008.2005752

55. Callen AL, Dupont SM, Pyne J, Talbott J, Tien P, Calabrese E, et al. The regional pattern of abnormal cerebrovascular reactivity in HIV-infected, virally suppressed women. *J Neurovirol.* (2020) 26:734–42. doi: 10.1007/s13365-020-00859-8
56. Chow FC, Wang H, Li Y, Mehta N, Hu Y, Han Y, et al. Cerebral Vasoreactivity evaluated by the breath-holding challenge correlates with performance on a cognitive screening test in persons living with treated HIV infection in China. *J Acquir Immune Defic Syndr.* (2018) 79:e101–4. doi: 10.1097/QAI.0000000000001805
57. Staszewski J, Debiec A, Skrobowska E, Stepień A. Cerebral Vasoreactivity changes over time in patients with different clinical manifestations of cerebral small vessel disease. *Front Aging Neurosci.* (2021) 13:727832. doi: 10.3389/fnagi.2021.727832
58. Mina Y, Wu T, Hsieh HC, Hammoud DA, Shah S, Lau CY, et al. Association of White Matter Hyperintensities with HIV status and vascular risk factors. *Neurology.* (2021) 96:e1823–34. doi: 10.1212/wnl.00000000000011702
59. Blair GW, Thrippleton MJ, Shi Y, Hamilton I, Stringer M, Chappell F, et al. Intracranial hemodynamic relationships in patients with cerebral small vessel disease. *Neurology.* (2020) 94:e2258–69. doi: 10.1212/wnl.00000000000009483
60. Hou X, Liu P, Li Y, Jiang D, De Vis JB, Lin Z, et al. The association between BOLD-based cerebrovascular reactivity (CVR) and end-tidal CO<sub>2</sub> in healthy subjects. *NeuroImage.* (2020) 207:116365. doi: 10.1016/j.neuroimage.2019.116365
61. Alsop DC, Detre JA, Golay X, Gunther M, Hendrikse J, Hernandez-Garcia L, et al. Recommended implementation of arterial spin-labeled perfusion MRI for clinical applications: a consensus of the ISMRM perfusion study group and the European consortium for ASL in dementia. *Magn Reson Med.* (2015) 73:102–16. doi: 10.1002/mrm.25197

## Glossary

cART	Combination antiretroviral therapy
PWH	People with HIV
HC	HIV negative healthy controls
CBF	Cerebral blood flow
CVR	Cerebrovascular reactivity
CBVD	Cerebrovascular disease
CSVD	Cerebral small vessel disease
CNS	Central nervous system
ASL	Arterial spin labeling
rs-fMRI	Resting-state functional magnetic resonance imaging
GFAP	Glial fibrillary acidic protein
BBB	Blood brain barrier
Shh	Sonic hedgehog
BSL	Baseline
W12	Week 12
Y2	Year 2
MND	Mild neurocognitive disorder
ANI	Asymptomatic neurocognitive impairment
MPRAGE	Magnetization-prepared rapid acquisition gradient echo
TR	Repetition time
TE	Echo time
pCASL	Pseudo continuous arterial spin labeling
ROI	Regions of interest
Amyg	Amygdala
CN	Caudate nucleus
GP	Globus Pallidus
Hippo	Hippocampus
PUT	Putamen
TH	Thalamus
PreC	Precuneus Cortex
GWM	Global white matter
BOLD	Blood oxygen dependent
BBR	Boundary-based registration
ICAM-1	Intracellular adhesion molecule 1
VCAM-1	Vascular cell adhesion molecule 1
MPs	Microparticles
SE	Standard error
PLD	Post label delay
M0	Equilibrium magnetization of arterial blood image